Fracture characterization from attenuation of Stoneley waves across a fracture

Sudhish K. Bakku, Michael Fehler and Daniel R. Burns, Earth Resource Laboratory, MIT*

SUMMARY

Fractures contribute significantly to the permeability of a formation. It is important to understand the fracture distribution and fluid transmissivity. Though traditional well logs can image fractures intersecting the borehole, they provide little information on the lateral extent of the fractures, away from the borehole, or the fluid transmissivity. Experiments in the past demonstrated that fracture compliance can be a good proxy to fracture fluid conductivity. We describe a method to estimate fracture compliance from the attenuation of Stoneley waves across a fracture. Solving the dispersion relation in the fracture, transmission coefficient of Stoneley waves across a fracture is studied over all frequency ranges. Based on the observations from the model, we propose that measuring the transmission coefficient near a transition frequency can help constrain fracture compliance and aperture. Comparing attenuation across a finite fracture to that of an infinitely long fracture, we show that a bound on the lateral extent of the fracture can be obtained. Given the limitation on the bandwidth of acoustic logging data, we propose using the Stoneley waves generated during micro-seismic events for fracture characterization.

INTRODUCTION

Fractures are one of the main conduits for fluid flow in the subsurface and characterizing them is important for economic production of hydrocarbons or geothermal energy. Borehole televiewer (BHTV) and formation micro imager (FMI) logs are the most popular tools for characterizing fractures intersecting boreholes, *in-situ*. These logs provide the location and orientation of fractures intersecting the borehole. However, from this data it is hard to differentiate between fractures with high or low fluid conductivity, and it is not possible to estimate the lateral extent of the fractures. Some of the fracture like features seen in the logs could be drilling induced. On the other hand, pressure transient tests can give an estimate of fluid conductivity. But, it is a macroscopic measurement averaging over a conducting region. On a reservoir scale, fracture networks are characterized by applying methods like amplitude variation with offset and azimuth (AVOA) (Sayers and Kachanov, 1995) and Scattering Index (Willis et al., 2006). AVOA estimates the anisotropy due to fracture sets, which is a function of fracture density, fracture compliance and orientation. This methodology is successful in determining the preferred fracture orientation but falls short in estimating the fracture density and compliance. Knowing the *in-situ* fracture compliance from borehole measurements, we may be able to estimate fracture density. The Scattering index method is suitable for larger discrete fracture networks and is based on analyzing the scattered coda from the fracture networks. Fang et al. (2012) estimated fracture spacing and orientation using a modified scattering index method. Numerical simulations (Grandi, 2008) show that intensity of scattering is proportional to the fracture compliance. Knowing the average fracture compliance of a region from borehole measurements we may be able to assign fracture compliance to regions away from borehole based on relative scattered energy. Moreover, previous lab studies (Pyrak-Nolte and Morris, 2000) suggest that fracture compliance and fluid conductivity are influenced by the same microscopic features and are related. In the future, fracture compliance can be a key link to estimate fracture conductivity and help us predict the permeability of the formation. In addition, fracture compliance can be a good measure to test the effectiveness of hydro-fracing. We can use compliance values to estimate the relative fluid transmissivity of different fractured zones. Thus, it is important to be able to estimate *in-situ* fracture compliance.

In this paper, we develop a model to study the attenuation of a Stoneley wave as it passes a fracture intersecting the borehole, to estimate fracture compliance and aperture, and constrain the lateral extent of fractures. Attenuation of Stoneley waves was studied earlier by Mathieu (1984), Hornby et al. (1989), Tang and Cheng (1993) and Kostek et al. (1998a,b). Mathieu (1984) assumed Darcy flow in the fracture, a low frequency approximation, and studied attenuation of Stoneley waves across the fracture. However, the assumption of Darcy flow is not valid for typical logging frequencies. Hornby et al. (1989) and Tang and Cheng (1993) solved the problem under a high-frequency approximation, which is a valid assumption for kHz range of frequencies. Later, Kostek et al. (1998b) extended the theory to include the elasticity of the formation. None of the studies above accounted for the fracture compliance that plays an important role in the Stoneley wave attenuation. We study Stoneley wave attenuation over all frequency ranges, considering the effects of fracture compliance.

THEORY

When Stoneley waves in a borehole cross a fracture intersecting the borehole, part of the energy is spent in pushing the fluid into the fracture and part of the energy is reflected at the interface. As a result, the transmitted wave is attenuated. The attenuation of the Stoneley wave depends on the amount of fluid squeezed into the fracture, which, in turn depends on the fracture transmissivity and compliance. We consider a circular horizontal fracture, of radius 'D' and intersecting a vertical borehole of radius R (see Figure 1). Due to the axial symmetry in the problem, we use cylindrical co-ordinates with 'r' denoting the radial distance from the center of the borehole, and z-axis along the borehole. The fracture top surface is located at z=0.

The pressure due to the incident Stoneley wave at the fracture

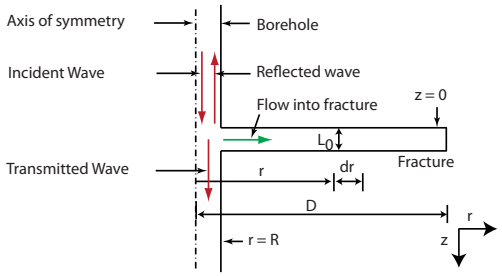

Figure 1: Schematic showing attenuation of Stoneley wave at a fracture intersecting a borehole.

top, z=0, $\overline{P_I}$, can be written as (Cheng and Toksöz, 1981)

$$\begin{aligned} \overline{P_I}(r,\omega) &= AI_0(fr) \\ f &= \frac{\omega}{c_t}\sqrt{1-\frac{c_t^2}{\alpha_f^2}} \end{aligned} \tag{1}$$

where, I_0 is the modified bessel function of the first kind and order zero, c_t is the phase velocity of the Stoneley wave, α_f is the acoustic wave velocity in the fluid, ω is the frequency of the incident Stoneley wave and A is a constant, respectively. The bar over the symbols denotes that the quantities are in the frequency domain. The variation of the pressure along the radial direction in the borehole is low for the range of frequencies of interest and we use the pressure averaged over the borehole radius as the measure for the remainder of the paper and denote it as $<\overline{P_I}>$. Pressure for the reflected Stoneley wave and transmitted Stoneley wave follow the same equation with different constants. We denote the pressure averaged over borehole radius for reflected and transmitted waves as $<\overline{P_R}>$ and $<\overline{P_T}>$, respectively. For continuity of pressure at z=0, we require that

$$<\overline{P_T}>=<\overline{P_I}>+<\overline{P_R}> \tag{2}$$

Also, conservation of mass requires that the flow due to the incident wave should be equal to the sum of flow due to the reflected wave, transmitted wave and the flow into the fracture. Expressing average flow as the product of cross section area and the average particle velocity, the mass conservation equation is given by

$$\begin{aligned} \pi R^2 <\overline{v_I}> &= \pi R^2 <\overline{v_R}> + \pi R^2 <\overline{v_T}> \\ &\quad + 2\pi R L_0 <\overline{v_F}(R)> \end{aligned} \tag{3}$$

where $<\overline{v_T}>$,$<\overline{v_I}>$,$<\overline{v_R}>$ are the particle velocities of the incident wave, reflected wave, and transmitted wave, respectively, averaged over the cross section. $<\overline{v_F}(R)>$ is the radial particle velocity in the fracture, at r=R, averaged over the fracture aperture. We assume that the flow into the fracture is driven by the pressure of the transmitted wave at the borehole wall, $\overline{P_T}(R)$. $<\overline{P_T}>$ and $\overline{P_T}(R)$ are related by (Mathieu, 1984)

$$\overline{P_T}(R) = \frac{fR}{2}\frac{I_0(fR)}{I_1(fR)} <\overline{P_T}> \tag{4}$$

where I_1 is the modified bessel function of the first kind and order one. We further define the acoustic impedance of the borehole, Z_B, and the impedance of the fracture, Z_F, as

$$\begin{aligned} Z_B &= \frac{<\overline{P_I}>}{<\overline{v_I}>} = \frac{<\overline{P_T}>}{<\overline{v_T}>} = \frac{<\overline{P_R}>}{<\overline{v_R}>} \\ Z_F &= \frac{<\overline{P_F}(R)>}{<\overline{v_F}(R)>} = \frac{<\overline{P_T}(R)>}{<\overline{v_F}(R)>} \end{aligned} \tag{5}$$

Solving equations 2 to 5, simultaneously, Mathieu (1984) obtained the transmission coefficient as

$$\frac{\overline{P_T}}{\overline{P_I}} = \frac{1}{1+X} \tag{6}$$

with

$$X = \frac{fL_0}{2}\frac{I_0(fR)}{I_1(fR)}\frac{Z_B}{Z_F} \tag{7}$$

where, $Z_B = \rho_f c_t$. He obtained Z_F by estimating flow into the fracture, assuming Darcy flow in the fracture, a low frequency approximation, and did not consider the effect of the fracture compliance. We estimate Z_F for arbitrary frequency and account for fracture complaince.

For simplicity, we assume the fracture to be a parallel plate with static aperture, L_0, and normal compliance, Z. Here, we neglect the effect of roughness, tortuosity and actual contact area of fracture on the fluid motion in the fracture. Fracture opening is proportional to the fracture compliance and the fluid pressure in the fracture, above static equilibrium. Fracture opening due to formation elasticity is negligible compared to that due to fracture compliance and is neglected. Thus, dynamic fracture aperture, $L(t)$, can be written as (Hardin et al., 1987)

$$L(t) = L_0 + ZP_F(t) \tag{8}$$

where $P_F(t)$ is the perturbation in the fracture fluid pressure due to fluid motion into the fracture. Fluid pressure and flow in the fracture are averaged over the aperture and only their radial variation is considered. The net flow out of a volume element, $2\pi rL(t)\,dr$, between r and $r+dr$ from the axis of the borehole, during a time increment dt, should equal the change in volume of the element, during the same time, due to perturbation in the aperture and the change in the fluid volume due to compressibility of the fluid. Thus, we arrive at

$$-\left(\frac{\partial q}{\partial r}+\frac{q}{r}\right) = \frac{dL}{dt} + L\gamma\frac{\partial P_F}{\partial t} \tag{9}$$

where γ is the fluid compressibility and q is the radial flow per unit length. Flow in the above equation can be related to the pressure gradient through dynamic conductivity, $\overline{C}$. Solving for the flow field in a rigid fracture, Tang (1990) showed that the flow averaged over the aperture at any location can be related to the radial pressure gradient at that location as

$$\overline{q} = -\overline{C}\frac{\partial\overline{P_F}}{\partial r}, \text{ where } \overline{C} = \frac{i\omega L_0}{k_r^2\alpha_f^2\rho_f} \tag{10}$$

where ρ_f is the fluid density and i is the imaginary unit. k_r is the radial wavenumber of those specific modes that can exist in the fracture and is obtained by solving the dispersion relation for the velocity field in the fracture (Tang, 1990). This

assumption is valid as long as the dynamic aperture is comparable to static aperture. After neglecting higher order terms, using equations 8, 9 and 10, we can write the differential equation for fluid pressure in the fracture in the frequency domain as

$$\frac{\partial^2 \overline{P_F}}{\partial r^2} + \frac{\partial \overline{P_F}}{\partial r} + \frac{k_r^2 \alpha_f^2}{\alpha_{eff}^2} \overline{P_F} = 0 \tag{11}$$

where $\alpha_{eff}^2 = \frac{1}{\rho_f} \frac{1}{(\gamma + \frac{Z}{L_0})}$, with boundary conditions:
1) At borehole radius, the pressure in the fracture should be equal to the transmitted wave, i.e., $\overline{P_F}(R) = \overline{P_T}(R)$. 2) At the fracture tip, $r = D$, fluid flow is zero and we require that $\frac{\partial \overline{P_F}}{\partial r} = 0$. The homogenous solutions to equation 11 are Hankel functions of first and second kind taking complex arguments. Taking these solutions and satisfying the boundary condition at the borehole and fracture tip, the pressure in the fracture can be written as

$$\overline{P_F}(r) = \overline{P_T}(R) \left[\frac{H_0^1(\zeta r) H_1^2(\zeta D) - H_1^1(\zeta D) H_0^2(\zeta r)}{H_0^1(\zeta R) H_1^2(\zeta D) - H_1^1(\zeta D) H_0^2(\zeta R)} \right] \tag{12}$$

where, $\zeta = \frac{k_r \alpha_f}{\alpha_{eff}}$ and H_m^n is the Hankel function of the nth kind and order m.

However, Tang (1990) showed that viscous or inertial forces dominate depending on the magnitude of the viscous skin depth, $\delta = \sqrt{\frac{2\nu}{\omega}}$, relative to the fracture aperture, L_0, where, ν is the kinematic viscosity of the fluid. Under the high frequency approximation ($\frac{\delta}{L_0} \ll 1$), the differential equation for pressure takes the form of a wave equation as the inertial forces dominate. Under the low frequency approximation ($\frac{\delta}{L_0} \gg 1$), the pressure follows a diffusion equation as the viscous forces dominate. For the frequencies of interest (0.5-2 kHz) in Full Waveform Acoustic Logging (FWAL) and for the range of natural fracture apertures (0.1-0.5 mm), the high frequency approximation is valid. However, Stoneley waves generated in a VSP setting can have lower frequency content. This motivates us to study the attenuation over the entire range of frequencies. In the transition zone, between the low and high frequency approximations, pressure has both wave and diffusive components. To address this, for an arbitrary frequency, we solved the dispersion relation numerically. The fundamental mode converged to the solutions predicted by Tang (1990) at high and low frequency limits. Taking this numerical solution for k_r, equation 12 encapsulates both diffusion and propagation. The contribution to flow by higher modes is negligible and only fundamental mode is considered in this study.

Knowing the distribution of pressure in the fracture from equation 12 and using equation 10, the radial flow into the fracture is given by

$$\begin{aligned} \overline{q}(R) &= \overline{P_T}(R) \zeta \frac{i\omega L_0}{k_r^2 \alpha_f^2 \rho_f} \\ &\times \left[\frac{H_1^1(\zeta R) H_1^2(\zeta D) - H_1^1(\zeta D) H_1^2(\zeta R)}{H_0^1(\zeta R) H_1^2(\zeta D) - H_1^1(\zeta D) H_0^2(\zeta R)} \right] \end{aligned} \tag{13}$$

Thus, the impedance of the fracture can be written as

$$\begin{aligned} Z_F &= \frac{< \overline{P_T}(R) >}{< \overline{v_F}(R) >} = \frac{< \overline{P_T}(R) >}{\overline{q}(R)/L_0} \\ &= \frac{k_r^2 \alpha_f^2 \rho_f}{i\omega\zeta} \\ &\times \left[\frac{H_0^1(\zeta R) H_1^2(\zeta D) - H_1^1(\zeta D) H_0^2(\zeta R)}{H_1^1(\zeta R) H_1^2(\zeta D) - H_1^1(\zeta D) H_1^2(\zeta R)} \right] \end{aligned} \tag{14}$$

From equations 6, 7 and 14 the transmission coefficient can be estimated.

To look at the effect of the finite size of fracture on the transmission coefficient, we compare the solution for a finite fracture with the solution for an infinitely long fracture. As $D \to \infty$, the ratio, $\frac{H_1^1(\zeta D)}{H_1^2(\zeta D)}$ approaches zero and the impedance of an infinitely long fracture, Z_F^∞, is given by

$$Z_F^\infty = \frac{k_r^2 \alpha_f^2 \rho_f}{i\omega\zeta} \frac{H_0^1(\zeta R)}{H_1^1(\zeta R)} \tag{15}$$

Taking zero fracture compliance and under the high frequency approximation, this solution matches the solutions given by Hornby et al. (1989) and Tang and Cheng (1993). The transmission coefficient, for an infinitely long fracture, is plotted against frequency for a given compliance and aperture in Figure 2(a). For comparison, the transmission coefficients under the low and high frequency approximation are plotted as well. At the low frequency limit, the transmission coefficient tends towards unity. With increasing frequency, the transmission coefficient decreases and reaches a minimum at the transition from low to high frequency and then increases with further increase in frequency. However, in high frequency regime, the transmission coefficient reaches a constant value. In general, as compliance increases, the transmission coefficient decreases over the entire frequency band (see Figure 2(b)). Thus, the transmission coefficient can be indicative of fracture compliance. For a given compliance, the location of the frequency having the minimum in the transmission coefficient depends on the viscosity of the fluid and the fracture aperture. Increasing viscosity pushes the minimum towards higher frequencies and larger aperture moves the minimum towards lower frequencies (see Figure 2(c)). Figure 2(d) shows transmission coefficients for a finite fracture case. The effect of the finite length of the fracture is to cause oscillations on top of the infinite fracture response. The period of these oscillations in the finite fracture case is dependent on the fracture compliance, fracture aperture and the length of the fracture and varies with frequency. The amplitude of these oscillations is larger at lower frequencies and approaches zero towards higher frequencies. At lower frequencies, the fluid pressure is perturbed deep into the fracture and the transmission coefficient is effected by the length of the fracture. At higher frequencies, the perturbation doesn't go deep into the fracture and we cannot differentiate between finite and infinite fracture cases. Thus, the frequency at which the finite length of the fracture effects the transmission coefficient depends on the length of the fracture. For this reason, in Figure 2(d), as D is increased from 0.5 m to 8 m, the finite fracture response matches the infinite

fracture response increasingly towards lower frequencies. Z_F^{∞} and Z_F are within 1%, when $|\frac{H_1^1(\zeta D)}{H_1^2(\zeta D)}| < 0.01$. Simplifying the ratio, we can show that this condition is satisfied at frequencies such that

$$\omega > 2.5 \frac{L_0}{\delta} \frac{\alpha_{eff}}{D} \tag{16}$$

In other words, to be able to estimate the length of a finite fracture, the data should have frequency content lower than that given by 16. For example, taking values for aperture as 500 μm and compliance as 10^{-10} m/Pa (all other parameters correspond to Figure 2), we need frequencies lower than 400 Hz, 17 Hz and 4 Hz to be able to detect finite fractures of length 1 m, 5 m and 10 m, respectively. Since the data are band limited we have constraints on how long a fracture we can detect.

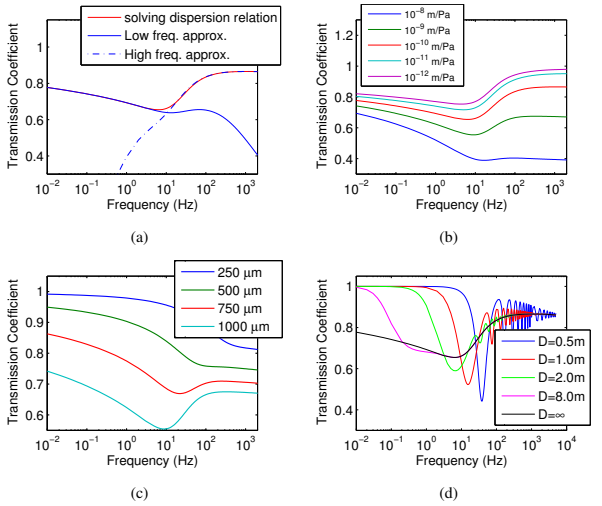

Figure 2: Transmission coefficient ($|P_T/P_I|$) is plotted against frequency. (a) High and low frequency approximation solutions are shown when $L_0 = 1mm$ and $Z = 10^{-10} m/Pa$. (b) Compliance is varied keeping aperture constant at 1 mm. (c) Aperture is varied for a constant compliance of $10^{-10} m/Pa$. (a),(b),(c) are obtained for an infinitely long fracture. (d) Solution for finite fracture case when the size of the fracture, D, is varied. Here, $L_0 = 1mm$ and $Z = 10^{-10} m/Pa$. All other parameters for the above studies are taken as 2R=15 cm, $\alpha_f = 1300 m/s$,$\alpha = 4500 m/s$,$\beta = 2650 m/s$, $\rho_f = 900 kg/m^3$,$\rho_s = 2400 kg/m^3$, $\nu = 10^{-5} m^2/s$. The fluid properties correspond to crude oil.

FRACTURE CHARACTERIZATION

We observe that the transition frequency of the transmission coefficients depends only on fracture aperture and fluid viscosity. Since the fluid viscosity is known, by determining the transition frequency from the field data we can constrain the fracture aperture. Fixing the fracture aperture, we can estimate the compliance value that fits the observed transmission coefficient in the high frequency regime. As we discussed, finite fracture effects are suppressed at higher frequencies and we need not know the fracture length to estimate compliance. Knowing fracture aperture and compliance, we can simulate the transmission coefficients for the infinite fracture case and compare it with the data. The frequency at which the data deviates from the expected infinite fracture response by a given margin, based on the accuracy of measurements, can be used to estimate fracture length by using an equation similar to 16. In the absence of data spanning over a range of frequencies from 10s of Hz to 1 kHz, the transmission coefficients observed in the high frequency regime can be explained by a range of possible combinations of aperture and compliance. However, if we assume a large aperture, we can constrain the minimum compliance required to have the observed attenuation as described in Bakku et al. (2011).

Currently, we can record at most as low as 500 Hz in a FWAL setting. This sets some limitations on the application of this theory to well log data. However, we could collect low frequency data when tube waves are excited in the borehole in a VSP setting (Bakku et al., 2011). Micro-seismic events accompanying hydraulic fracturing are reported to have a frequency band ranging from as low as 30 Hz (Fehler and Phillips, 1991) to kHz (Song and Toksoz, 2011). Similarly, micro-seismic events generated during production have low frequency content (on the order of 10s of Hz). We propose that the Stoneley waves excited in the boreholes during micro-seismic events can be used to characterize the fractures. This information can also be used to evaluate the performance of hydraulic fracturing procedures.

The effect of fracture compliance on attenuation of Stoneley waves is not negligible and conclusions from previous models should be revisited. A compliant single fracture can explain low transmission coefficients without demanding unrealistic apertures as reported by Hornby et al. (1989).

CONCLUSIONS

Attenuation of Stoneley wave across a fracture in a borehole is modeled accounting for the intrinsic fracture stiffness of the fracture. The pressure field in the fracture was solved without any low/high approximations on frequency. Thus, transmission coefficients over a range of frequencies and fracture compliances were analyzed. The transmission coefficient has a minimum at a transition frequency that decreases with increasing compliance. It is observed that measurements taken near the transition frequency can constrain compliance and aperture better. Under the high frequency approximation we can find a lower bound on compliance. Finite length of the fracture causes frequency dependent deviation in the transmission coefficient from the infinite fracture response. This observation allows the lateral extent of a finite fracture to be estimated.

ACKNOWLEDGEMENTS

This work was funded by the Eni Multiscale Reservoir Science Project within the Eni-MIT Energy Initiative Founding Member Program.

REFERENCES

Bakku, S. K., M. Fehler, and D. R. Burns, 2011, Estimation of fracture compliance from tubewaves generated at a fracture intersecting a borehole: SEG Technical Program Expanded Abstracts, **30**, 1819–1824.

Cheng, C. H., and M. N. Toksöz, 1981, Elastic wave propagation in a fluid-filled borehole and synthetic acoustic logs: Geophysics, **46**, 1042.

Fang, X., M. Fehler, Z. Zhu, Y. Zheng, and D. Burns, 2012, Reservoir fracture characterizations from seismic scattered waves: SEG expanded abstract.

Fehler, M., and W. S. Phillips, 1991, Simultaneous inversion for q and source parameters of microearthquakes accompanying hydraulic fracturing in granitic rock: Bulletin of the Seismological Society of America, **81**, 553–575.

Grandi, S., 2008, Multiscale determination of in situ stress and fracture properties in reservoirs: Ph.D thesis, MIT.

Hardin, E. L., C. H. Cheng, F. L. Paillet, and J. D. Mendelson, 1987, Fracture characterization by means of attenuation and generation of tube waves in fractured crystalline rock at Mirror lake, New Hampshire: Journal of Geophysical Research, **92**, 7989–8006.

Hornby, B. E., D. L. Johnson, K. W. Winkler, and R. A. Plumb, 1989, Fracture evaluation using reflected stoneley-wave arrivals: Geophysics, **54**, 1274–1288.

Kostek, S., D. L. Johnson, and C. J. Randall, 1998a, The interaction of tube waves with borehole fractures, part I: Numerical models: Geophysics, **63**, 800–808.

Kostek, S., D. L. Johnson, K. W. Winkler, and B. E. Hornby, 1998b, The interaction of tube waves with borehole fractures, part II: analytical models: Geophysics, **63**, 809–815.

Mathieu, F., 1984, Application of full waveform acoustic logging data to the estimation of reservoir permeability: M.S. thesis, MIT, Cambridge.

Pyrak-Nolte, L., and J. Morris, 2000, Single fractures under normal stress: The relation between fracture specific stiffness and fluid flow: International Journal of Rock Mechanics and Mining Sciences, **37**, 245–262.

Sayers, C. M., and M. Kachanov, 1995, Microcrack-induced elastic wave anisotropy of brittle rocks: Journal of Geophysical Research, **100**, PP. 4149–4156.

Song, F., and M. N. Toksoz, 2011, Full-waveform based complete moment tensor inversion and source parameter estimation from downhole microseismic data for hydrofracture monitoring: Geophysics, **76**, WC103–WC116.

Tang, X., 1990, Acoustic logging in fractured and porous formations: Ph.D thesis, MIT, Cambridge.

Tang, X. M., and C. H. Cheng, 1993, Borehole stoneley wave propagation across permeable structures: Geophysical Prospecting, **41**, 165–187.

Willis, M. E., D. R. Burns, R. Rao, B. Minsley, M. N. Toksöz, and L. Vetri, 2006, Spatial orientation and distribution of reservoir fractures from scattered seismic energy: Geophysics, **71**, O43–O51.